PERGAMON

Journal of Structural Geology 24 (2002) 173–192

JOURNAL OF STRUCTURAL GEOLOGY

www.elsevier.com/locate/jstrugeo

Geometry and structure of northern surface ruptures of the 1999 Mw = 7.6 Chi-Chi Taiwan earthquake: influence from inherited fold belt structures

Jian-Cheng Lee[a,*], Hao-Tsu Chu[b], Jacques Angelier[c], Yu-Chang Chan[a], Jyr-Ching Hu[d], Chia-Yu Lu[e], Ruey-Juin Rau[f]

[a]*Institute of Earth Sciences, Academia Sinica, P.O. Box 1-55, Nankang, Taipei, Taiwan, ROC*
[b]*Central Geological Survey, P.O. Box 968, Taipei, Taiwan, ROC*
[c]*Tectonique Quantitative, Département de Géotectonique and ESA 7072, Université P.-&-M. Curie, Paris, France*
[d]*The Institute for Secondary School Teacher of Taiwan, Taichung, Taiwan, ROC*
[e]*Department of Geology, National Taiwan University, Taipei, Taiwan, ROC*
[f]*Department of Earth Sciences, National Cheng-Kung University, Tainan, Taiwan, ROC*

Received 1 September 2000; revised 15 March 2001; accepted 20 March 2001

Abstract

Surface ruptures associated with the 1999 Mw = 7.6 Chi-Chi earthquake in central western Taiwan have been characterised by mapping along the northern fault-segment. The earthquake occurred on the reactivated Chelungpu fault in the frontal portion of the thin-skinned Taiwan fold-and-thrust belt. The N–S trending Chelungpu fault is a 90-km-long major west-verging thrust, which principally slips within, and parallel to, bedding of the Pliocene Chinshui Shale. In the northern segment of the earthquake fault trace, that we name the Shihkang–Shangchi fault zone, the surface ruptures turn to an E–W strike and produce a series of thrust-and-backthrust pop-ups, about 15 km long, forming several discontinuous subsegments distributed within a broad regional Pliocene syncline.

The northern fault segments activated during the Chi-Chi earthquake, in the area where the displacement is largest, not only display anomalous trends and a variety of mechanisms, but also raise a major problem of structural inheritance. Detailed field investigation and kinematic analysis indicate that the surface ruptures in the Shihkang–Shangchi fault zone are the result of dip-slip thrusting, occasionally with a minor strike-slip component. The surface ruptures emerge at the surface from bedding-parallel thrusts on both limbs of the regional south-plunging syncline. In the middle part of the syncline, bedding-parallel thrusts are connected by thrusts that cross-cut beds. The surface ruptures also reactivate a NE–SW trending anticline (Diaoshenshan), with west-vergent thrust on the backlimb and east-vergent backthrust on the forelimb. This anticline is undergoing uplift by breaking through the regional N–S trending syncline.

Combining GPS measurements, seismological data, and geological analyses, we propose a kinematic model with a 3-D fault surface for the 1999 earthquake in the area of the northern termination. We highlight the influence of both the local and regional structures (bedding parallel slip, pre-existing faults and folds) on the development of the earthquake rupture, and hence the role of the structural inheritance. We conclude that the south-plunging regional Pliocene syncline in fact acts as a slip/strain guide for the northern termination of the Chelungpu thrust. The Pliocene Chinshui Shale, as a major source of weakness within the syncline, has strongly influenced the pattern of slip surface during the 1999 earthquake rupture. We interpret the large vertical displacement along the northern segment as the fault rupture occurring over a surface whose radius of curvature tightens toward the north around the core of the syncline.

Keywords: Chi-Chi earthquake; Fault; Fold-and-thrust belt; Taiwan

1. Introduction

The Chi-Chi earthquake occurred at 1:47 local time on 21 September 1999 (17:47 GMT on 20 September) in central western Taiwan (Fig. 1). It is the largest earthquake (Mw = 7.6) that has occurred in Taiwan in this century (Chung and Shin, 1999; IES, 1999; Ma et al., 1999; Kao and Chen, 2000). About 2400 people lost their lives due to the earthquake, and economic losses are estimated at 14 billion US dollars. The epicenter of the earthquake (latitude 23°50′22″N and longitude 121°49′50″E) is located 15 km east of the leading edge of the thrust belt, with a focus at a depth of about 5–10 km (Chung and Shin, 1999; IES, 1999; Ma et al., 1999; Chang et al., 2000; Kao and Chen, 2000)

* Corresponding author. Tel.: +886-2-27839910, x409; fax: +886-2-2783 9871.
E-mail address: jclee@earth.sinica.edu.tw (J.-C. Lee).

0191-8141/02/$ - see front matter
PII: S0191-8141(01)00056-6

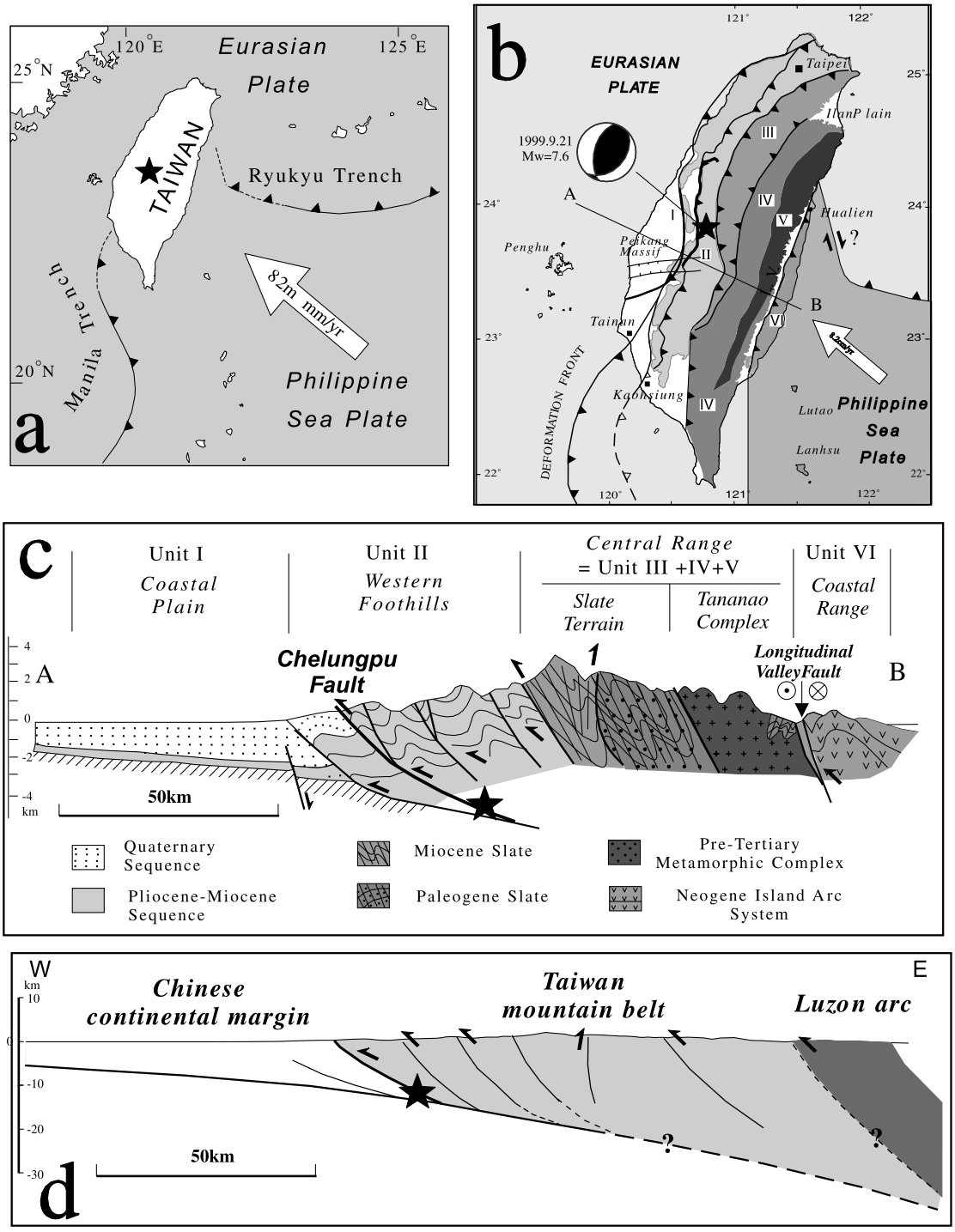

Fig. 1. (a) Tectonic framework of Taiwan and location of the 1999 Mw = 7.6 Chi-Chi earthquake. (b) General geological map of Taiwan, with the epicentre of the Chi-Chi earthquake. Rock units I to V belong to the Eurasian plate. I: Coastal plain, II: Foothills, III: Hsuehshang Range, IV: Backbone Range, V: Tananao metamorphic basement; Rock unit VI, Coastal Range, belongs to the Philippine Sea plate. (c) General geological cross-section of the Taiwan mountain belt along line a–b. The Chi-Chi earthquake ruptured the Chelungpu fault on the frontal thin-skinned fold-and-thrust zone of the mountain belt. (d) Schematic structure at upper-crust scale across the Taiwan mountain belt.

Numerous aftershocks, including an event of Mw = 6.4 (Kao and Chen, 2000), were distributed around the main shock (particularly to the east) in a large area of central Taiwan (Fig. 2).

The Chi-Chi earthquake ruptured a major reverse fault, the Chelungpu fault (Bilham and Yu, 1999; Central Geological Survey, 1999a; IES, 1999). The Chelungpu fault trends N–S to NNE–SSW and is one of the major thrust faults at the mountain front of the fold-and-thrust belt of Taiwan (Fig. 1c; Elishewitz, 1963; Ho, 1967, 1976; Biq,

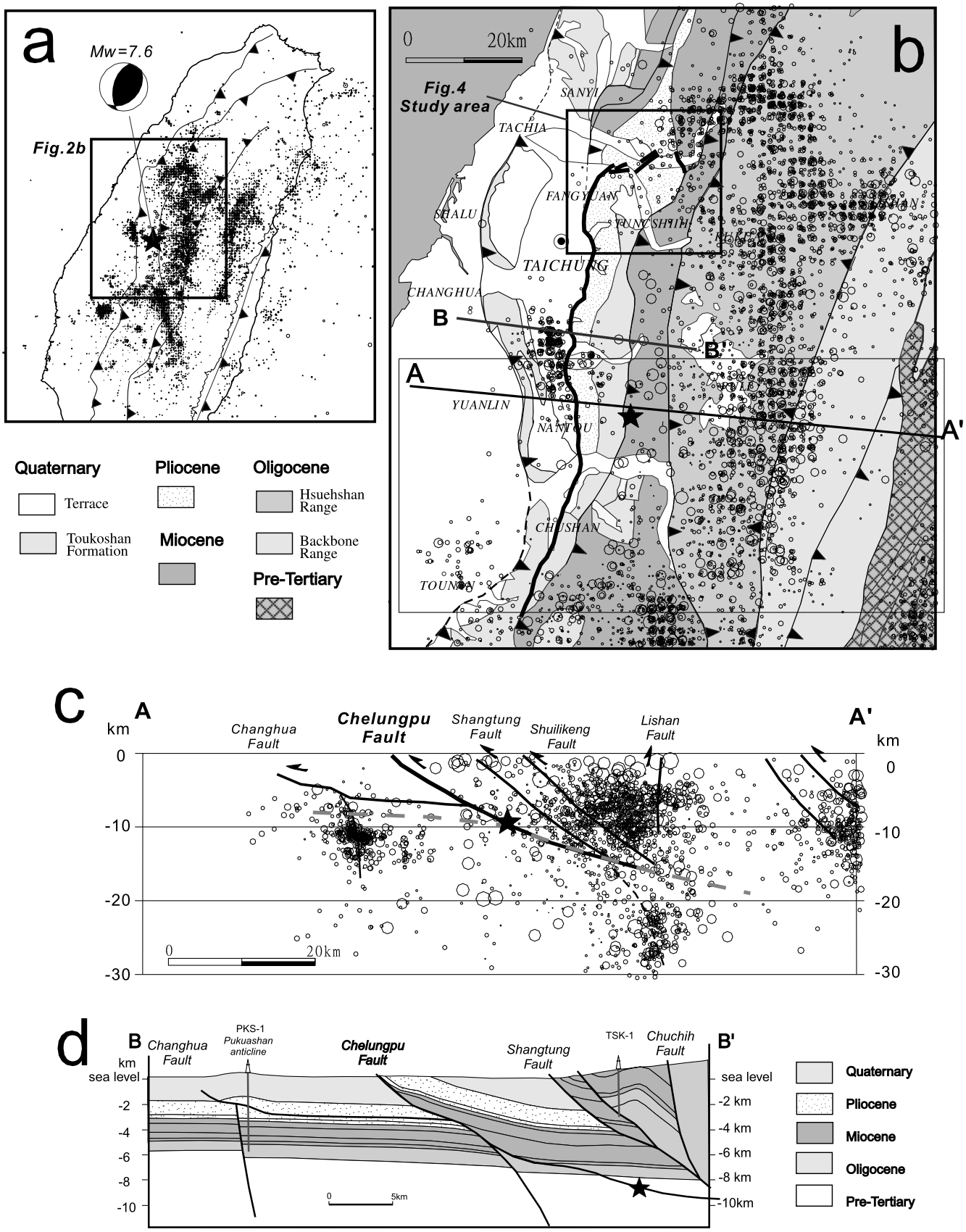

Fig. 2. Seismicity maps (a) (b) and cross-sections (c) (d) of the 1999 Mw = 7.6 Chi-Chi earthquake. The mainshock is shown by the star. The focal mechanism solution of the mainshock is based on the broadband network of Taiwan (Kao and Chen, 2000). The aftershocks (from 21/9/1999 to 28/2/2000) are shown by circles. Geological balanced cross-section (d) (after Angelier et al. (2000), based on an original balanced cross-section by Mouthereau et al. (2001)) shows that a hanging wall flat of Pliocene strata is thrusted over a footwall flat of Quaternary deposits.

1972; Suppe, 1980; Namson, 1981; Lee et al., 1996; Mouthereau, 2000). The earthquake produced a nearly continuous surface rupture 80–90 km long from south to north. The surface ruptures generally trend N–S, closely following the mapped trace of the Quaternary Chelungpu fault scarp, which separates Miocene–Pliocene strata of the foothills belt from late Quaternary sediments deposited in the coastal plain of western Taiwan (Fig. 2). However, the northern termination of the surface ruptures rotates clockwise almost 90° to an E–W trend, then stops abruptly. The seismological inversion shows that the 1999 rupture initiated in the south and propagated towards the north (Kikuchi et al., 2000; Kao and Chen, 2000; Lee and Ma, 2000; Ma et al., 2000). Coseismic movement from GPS measurement (Central Geological Survey, 1999b; IES, 1999; Yang et al., 2000; Yu et al., 2001) shows a northward increase of horizontal displacement from 2–3 m in the south to 7–9 m in the north along the Chelungpu fault (Fig. 3), which is also consistent with the northward propagation from the above seismic study. Displacement on the N–S segment of the surface rupture generally ranged from 2–6 m of vertical throw, with greater slip towards the northern end of the fault. Vertical displacement up to 8–10 m occurred at the northwestern corner of the rupture. Minor lateral movement with 1–3 m horizontal displacement could also be observed along the surface faults at a few sites, especially in the small subsegments of the transfer zones, whose locations usually correspond to the mouth of the rivers (Lee et al., 2001). The surface ruptures revealed, in terms of fault geometry and structure, thrust behaviour with a slight left-lateral component.

Several problems concerning the northern surface ruptures (hereafter named the Shihkang–Shangchi fault zone) deserve attention. For instance, why did the trend of the surface faults change so abruptly in the northern segment of the earthquake rupture (i.e. N–S trend to E–W trend)? Why were the displacements generally larger in this northern termination than along the main segment of the Chelungpu fault? How did the surface rupture of the earthquake propagate and terminate towards the north? Why did the surface rupture stop in the Shihkang–Shangchi zone? Were these complex earthquake surface ruptures guided by local specific geological features? Is there any correlation between the pattern of the earthquake surface ruptures and the regional geology/tectonics? To answer these questions, we carried out a structural geological survey in order to understand both the geometry of the northern surface ruptures and their relation to geological structures in this area. We paid particular attention not only to the structural pattern of the earthquake rupture and the pre-existing features, but also to the kinematics of faulting as revealed by slip indicators in the field, including earthquake-related striations on fault surfaces. In some cases, we could reconstruct the kinematics of brittle deformation by using stress tensor inversion of slip data (Angelier, 1984, 1989, 1994), although the lack of variety in fault orientations resulted in a major limitation in this analysis. Although our primary observations came from geological field investigations, we also took into consideration the available geological, seismological, and geodetic information.

Other examples of thrust-related earthquakes in fold belts in the past decades have been presented in the literature, including the 1978 Mw = 7.7 Tabas-e-Golshan earthquake (Berberian, 1979), the 1980 Mw = 7.3 El Asnam earthquake (Philip and Meghraoui, 1983), the 1983 Mw = 6.5 Coalinga earthquake (Stein and King, 1984), the 1988 Mw = 7.0 Spitak earthquake (Philip et al., 1992), and more recently the 1994 Mw = 6.7 Northridge earthquake (Tsutsumi and Yeats, 1999). Surface ruptures related to pre-existing faults or regional geological structures have been discussed to some extent, particularly for earthquakes in Southern California. For example, Tsutsumi and Yeats (1999) have identified the surface expression of fault-propagation folding related to the 1994 Northridge earthquake, Shaw and Shearer (1999) have shown detailed surface structures related to the blind thrust of the 1987 Whittier Narrows earthquake, and Mueller and Suppe (1997) indicated geomorphic evidence for fault-bend folding during the 1952 Arvin-Tehachepi earthquake. The 1999 Chi-Chi earthquake ruptured a surface break about 90 km long in a fold-and-thrust belt with extensive surface geological data and subsurface geological/geophysical data of deep wells and seismic reflection profiles. This earthquake gives us an excellent opportunity to study the geometrical and structural relationship between the earthquake fault and the geological structure in detail.

We have carried out detailed field investigations along the northern surface ruptures of the 1999 Chi-Chi earthquake during the six months, especially the first month, after the earthquake. In this paper, we describe the characteristics of the northern segment of the surface ruptures, present a kinematic analysis of the surface faulting based on outcrop measurements in the field, and interpret the northern surface ruptures in terms of structural inheritance. We first present the regional geology and its significance relative to the earthquake fault, then describe the structural features of the northern surface ruptures of the 1999 Chi-Chi earthquake, and present the kinematics analysis of displacements on fault scarps. We also present a serial cross-section along the zone of the northern surface ruptures in order to reveal its along-strike variation. A kinematic model with a 3-D geometry of the 1999 earthquake fault surface is then presented to illustrate the close relationship between the geometry of the inherited regional geological structure and the northern termination of the surface breaks.

2. Geological constraints

The 1999 Chi-Chi earthquake is the seismological manifestation of active shortening in the Taiwan fold-and-thrust belt (Fig. 1), produced by the Plio-Pleistocene subduction of

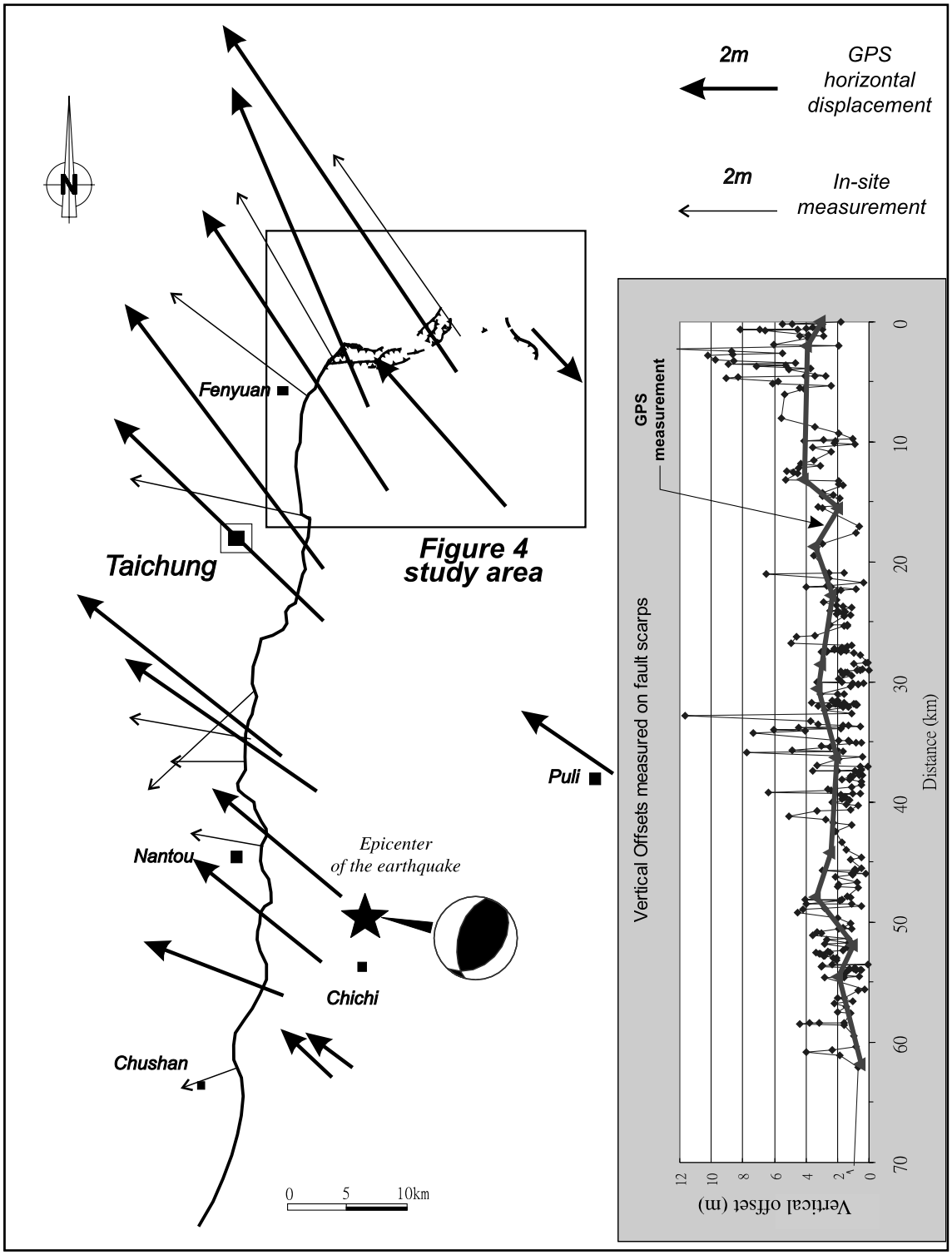

Fig. 3. Kinematics data of the 1999 Chi-Chi earthquake. The thin arrows represent the horizontal displacements obtained from the in-site outcrop measurements (Lee et al., 2001). The heavy arrows indicate the horizontal displacements of the near-fault GPS coseismic measurements (Central Geological Survey, 1999b; IES, 1999; Yang et al., 2000; Yu et al., 2001). The diagram to the right shows the along-strike variation of the vertical offsets measured directly on fault scarps and calculated from the GPS measurement, respectively. Both horizontal and vertical displacements increased from south to north along the surface ruptures. The orientations of the horizontal displacements for the GPS data and the outcrop measurements both reveal a substantial clockwise rotation from south to north.

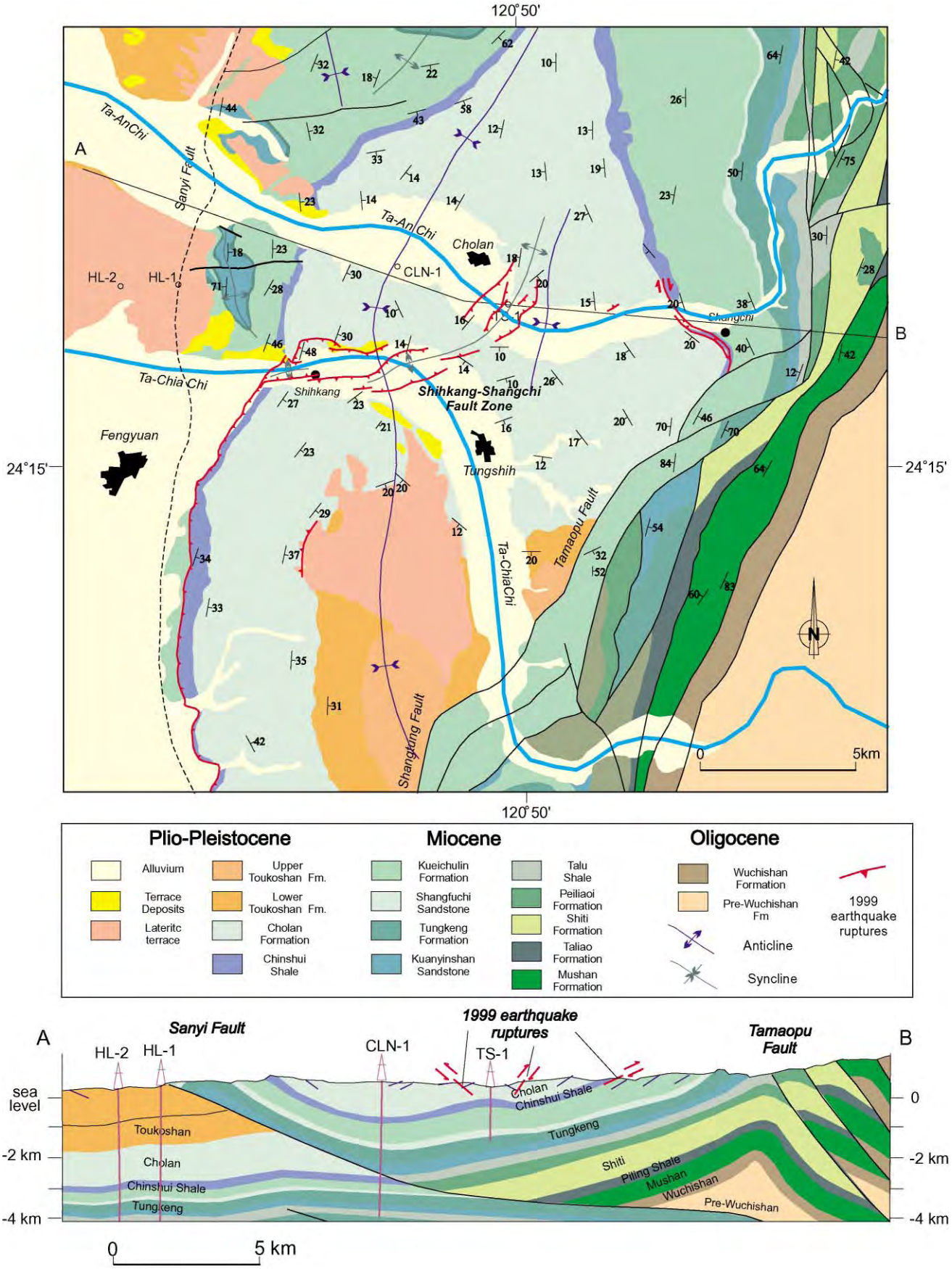
120°50'
24°15'
A
B
Ta-AnChi
Sanyi Fault
Ta-AnChi
Cholan
CLN-1
HL-2
HL-1
Shangchi
Ta-Chia Chi
Shihkang
Shihkang-Shangchi Fault Zone
Fengyuan
Tungshih
Tamaopu Fault
Ta-ChiaChi
Shangtung Fault
N
0
5km
Plio-Pleistocene
Alluvium
Terrace Deposits
Lateritc terrace
Upper Toukoshan Fm.
Lower Toukoshan Fm.
Cholan Formation
Chinshui Shale
Miocene
Kueichulin Formation
Shangfuchi Sandstone
Tungkeng Formation
Kuanyinshan Sandstone
Talu Shale
Peiliaoi Formation
Shiti Formation
Taliao Formation
Mushan Formation
Oligocene
Wuchishan Formation
Pre-Wuchishan Fm
Anticline
Syncline
1999 earthquake ruptures
A
B
Sanyi Fault
1999 earthquake ruptures
Tamaopu Fault
HL-2
HL-1
CLN-1
TS-1
sea level
-2 km
-4 km
Toukoshan
Cholan
Chinshui Shale
Tungkeng
Cholan
Chinshui Shale
Tungkeng
Shiti
Piling Shale
Mushan
Wuchishan
Pre-Wuchishan
0
5 km

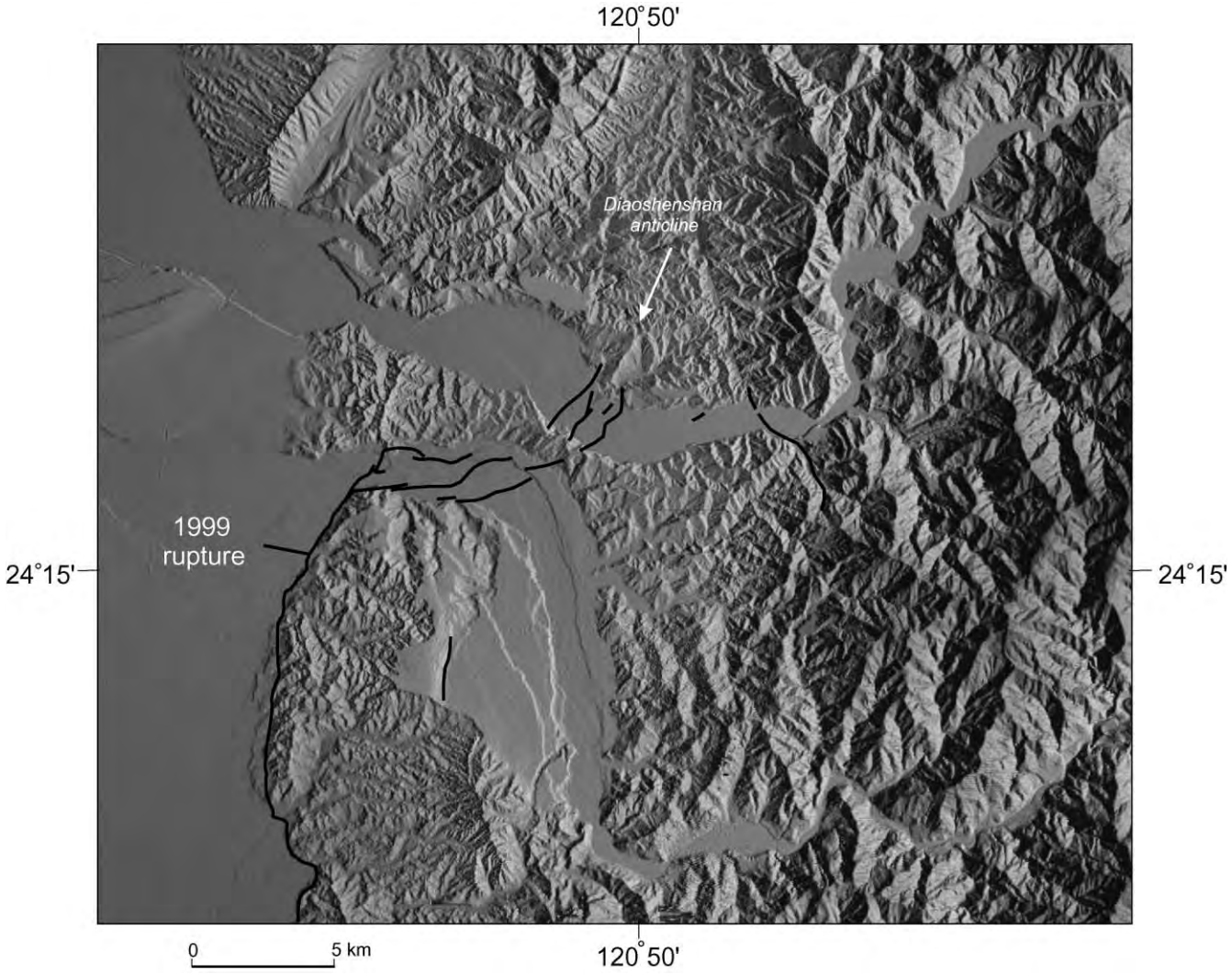

Fig. 5. 40-m DEM shading image of the northern termination area of the 1999 earthquake. Location is the same as geological map of Fig. 4. The NE–SW trending Diaoshenshan anticline fold is clearly visible in the rapidly eroded regional syncline with low topographic relief. This indicates that the Diaoshenshan anticline is an active uplift structure.

the Eurasian plate beneath the Philippine Sea plate (Ho, 1975, 1986; Suppe, 1981). The main segment of the surface rupture produced in the earthquake closely followed the mapped trace of the Chelungpu fault (Chinese Petroleum Corporation, 1974, 1982; Central Geological Survey, 1999b), along which the Pliocene marine sediments of the Chinshui Shale are overthrust onto Holocene alluvium (Fig. 2). The surface ruptures coincide with the geomorphic and geologic contact that separates rapidly eroded foothills underlain by Mio-Pliocene sediments and flat-lying late Quaternary alluvium in the foreland basin (Fig. 2). The Pliocene sediments of the Chinshui Shale and the overlying Cholan Formation are exposed in the hanging wall of the thrust and dip gently 20–40° to the southeast (Fig. 2d). The Chelungpu fault consists of a hanging-wall flat thrusting over a footwall ramp. The slip generally developed parallel to bedding in the Chinshui Shale. The Chinshui Shale is composed of 150–200 m of greyish fine-grained shale or mudstone (Chang, 1971; Chou, 1971), which is a mechanically appropriate weak material for the development of a major fault zone.

In the case of the northern termination in the Shihkang–Shangchi fault zone (SSFZ) (Fig. 4), the surface ruptures departed from the Chelungpu fault and turned northeast into the hills. Although the ruptures in the SSFZ did not follow a single, relatively planer fault surface (as the main segment

Fig. 4. General geological map (after Chinese Petroleum Corporation 1:100,000 scale map) and corresponding geological cross-section in the Shihkang–Shangchi fault zone. The surface ruptures of the 1999 Chi-Chi earthquake were limited by the Chinshui Shale on both sides within the regional south-plunging Pliocene syncline.

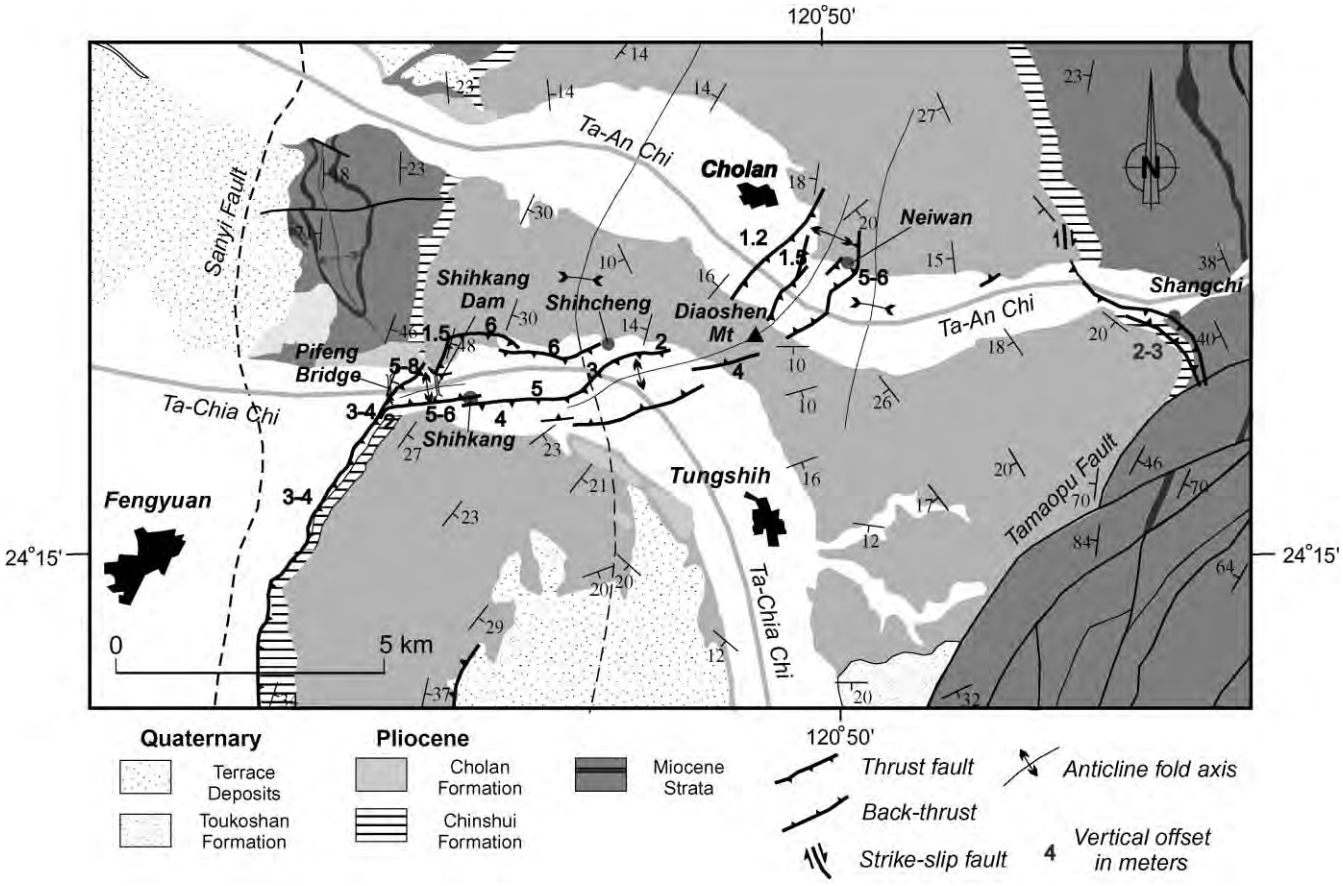

Fig. 6. Map of the northern surface ruptures of the 1999 Chi-Chi earthquake in the Shihkang–Shangchi fault zone. The vertical displacements observed on the fault scarps have been shown as numbers on the map. Note that the earthquake surface faults as well as the local young folding structures (trending E–W to NE–SW) within the Cholan Formation have obliquely cut across the regional old anticlinal and synclinal fold structures (trending N–S).

of the Chelungpu rupture trace did), they correspond to geomorphic features, such as topographic scarps, fold axes, and stream valleys. These geomorphic features (e.g. the Diaoshenshan anticline) are clearly visible on the 40 m DEM image (Fig. 5) in the low relief surface of the syncline area where the Mio-Pliocene formations crop out. We argue that such a low relief cannot be a simple remnant of the fault-bend fold formed above the Chelungpu thrust in its early stage of development. Rather, it represents the relief produced in the current phase of uplift. Based on our mapping of the 1999 fault traces in this area and considering their close relationship with the relief, we conclude that the ruptures along the SSFZ followed and reactivated pre-existing geological structures, which exhibit active geomorphic features. Northwest-verging thrusts with south-east-verging backthrusts are the most characteristic structures.

From a structural standpoint, it is quite significant that the SSFZ developed within Pliocene strata of an open synclinal fold (Fig. 4). The 1999 fault has a simpler structure to the south where the thrust makes a clean surface break (Fig. 2d), and a new lateral ramp is forming farther north that cuts across bedding of strata (Fig. 4). This northern new lateral ramp represents an on-going fault which is breaking-through a regional syncline. At a wider scale, the structural configuration along the Chelungpu fault can be summarized as follows. The Plio-quaternary strata hanging wall of the Chelungpu fault has a quite different structure to the south and to the north: a N–S trending monocline with an eastward dip of about 20–40° in the south and the large syncline already described in the north (Fig. 2). This difference of regional structural inheritance exerted an important influence on the development of the earthquake surface breaks, because the earthquake rupture occurred essentially along the mechanically weak beds of the Chinshui Shale in the uppermost few kilometres of the sedimentary pile. As a consequence, to the south, along the main segment of the Chelungpu fault, the surface rupture mainly involved widespread bedding-parallel thrusting along the Chinshui Shale, on the western side of the monocline. In contrast, the northern segment underwent a more complex pattern of deformation, combining across-bedding and bedding-parallel deformation styles as a function of the local structure.

On one hand, the earthquake faulting in the northern area often took place within the Chinshui Shale as a bedding

thrust on both the limbs of the large syncline, despite the orientation of the syncline axis and the strikes of the strata that displayed large obliquity with respect to the motion vector. On the other hand, and because of this obliquity, the earthquake fault also acted as a bedding-cut-through thrust. This is typically the case in the younger Cholan Formation, in the middle part of the Pliocene synclinal fold structure. In map view (Fig. 4), the fault rupture developed in the Chinshui Shale to the west, then turned clockwise into the Cholan Formation in the central area of the syncline, and finally turned clockwise again into the Chinshui Shale to the east. The distribution of the earthquake surface ruptures indicates strong correlation with the regional stratigraphy and structure (compare the strikes of the surface rupture segments and those of the bedding planes in the map of Fig. 4). We will discuss the structural control and geological inheritance with the development of the earthquake fault in the later section.

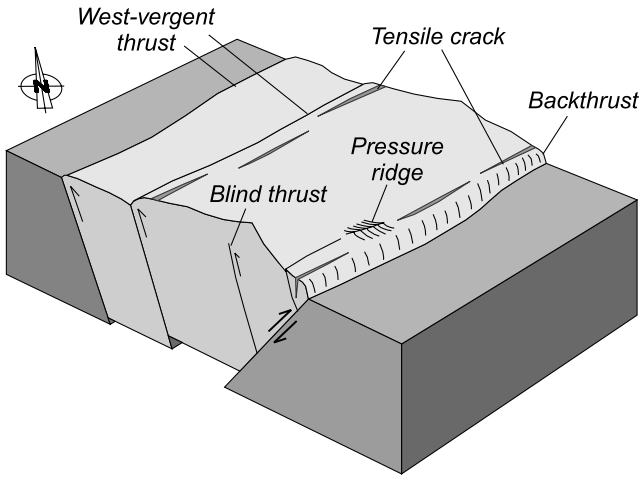

Fig. 7. General surface fault movement in a 3-D block diagram and common surface features observed in the Shihkang–Shangchi fault zone. The surface ruptures in the Shihkang–Shangchi fault zone are generally represented by a pop-up fold bounded by two opposite major faults of thrust and backthrust. Secondary structures, such as tensile cracks, can also be observed especially in the hanging wall of the earthquake fault.

3. General features of the northern surface ruptures

The northern termination of the 1999 surface ruptures occurred within the Pliocene syncline in a zone of complex deformation that trends NE–SW to E–W. The northern surface fault zone is approximately 1–2 km wide and extends about 15 km long from Shihkang towards Shangchi (Fig. 6). The surface ruptures of the Shihkang–Shangchi fault zone are discontinuous with a complex en échelon pattern and are composed of several parallel outwardly verging thrusts and backthrusts. These earthquake surface ruptures occurred principally on local pre-existing anticlines or other geological structures.

In contrast to many thrust displacement profiles, which show low displacement near the fault tips (Sieh and Jahns, 1984; Yeats et al., 1997), not only are the vertical offsets of the surface faults large in the northern segment (generally ranging 2–6 m and up to 8–10 m at some sites, Fig. 6), but they are also commonly larger than those observed along the main segment of the Chelungpu fault. The vertical displacement is generally greater than the horizontal component of slip. We interpret this to suggest that, at the near-surface level, the reverse faults in the SSFZ are steeper than the usual dip of the Chelungpu fault. This inference is also supported by local outcrop observations and measurements.

During the earthquake, thrust scarps accompanied by tensile cracks caused extensive damage within the northern surface rupture zone. One of the most spectacular damaged areas, at the Shihkang Dam, exhibited a vertical offset of 8–10 m on the main body of the dam. This large offset of the dam is not representative of the general behaviour of the fault. It should be interpreted as the local result of several combined deformational processes, which include two thrust ruptures, a backthrust fault, and pressure ridges (Chen et al., 2000; Lee et al., 2001), which together formed a complex deformation pattern in the core of an upright ENE-trending anticline (Fig. 6).

Fig. 7 illustrates the general features of the northern surface rupture. Individual surface faults are hundreds of metres to a few kilometres long and bound pop-up structures ranging from tens to hundreds of metres wide. Anticlines are usually present in the pop-ups. Other outcrop-scale features included tensile cracks, normal faults, and pressure ridges (Fig. 7). Tensile cracks are common along the thrust scarps where hanging wall blocks collapsed onto the ground surface (e.g. 1980 El Asnam earthquake, Philip and Meghraoui, 1983). Another common deformation feature was transpression or transtension structures located between overlapped fault segments, such as several extensional joints or fractures observed in the overstep zone in the Shihkang village.

Recognising the geometrical relationship between the earthquake surface breaks and the geological structure (or the morpho-structural features) is more difficult in the middle part of the SSFZ than that along the main segment of the Chelungpu fault where surface breaks occur along the range front. The surface ruptures in the middle part of the SSFZ developed within a large Pilocene synclinal structure that trends oblique to the Chelungpu fault, and they did not follow previously mapped geological faults. However, many of the surface faults developed along local morphological alignments such as for the topographic scarp in Shihkang, or geological structures like the anticline near Neiwan (Fig. 6). Thus, the relationship between the pre-existing geological structure and morphology certainly exists in the northern area, but it must be considered at a more local scale than to the south. It clearly appears that the development of the northern earthquake ruptures was strongly dependent on the pre-existing geological structure.

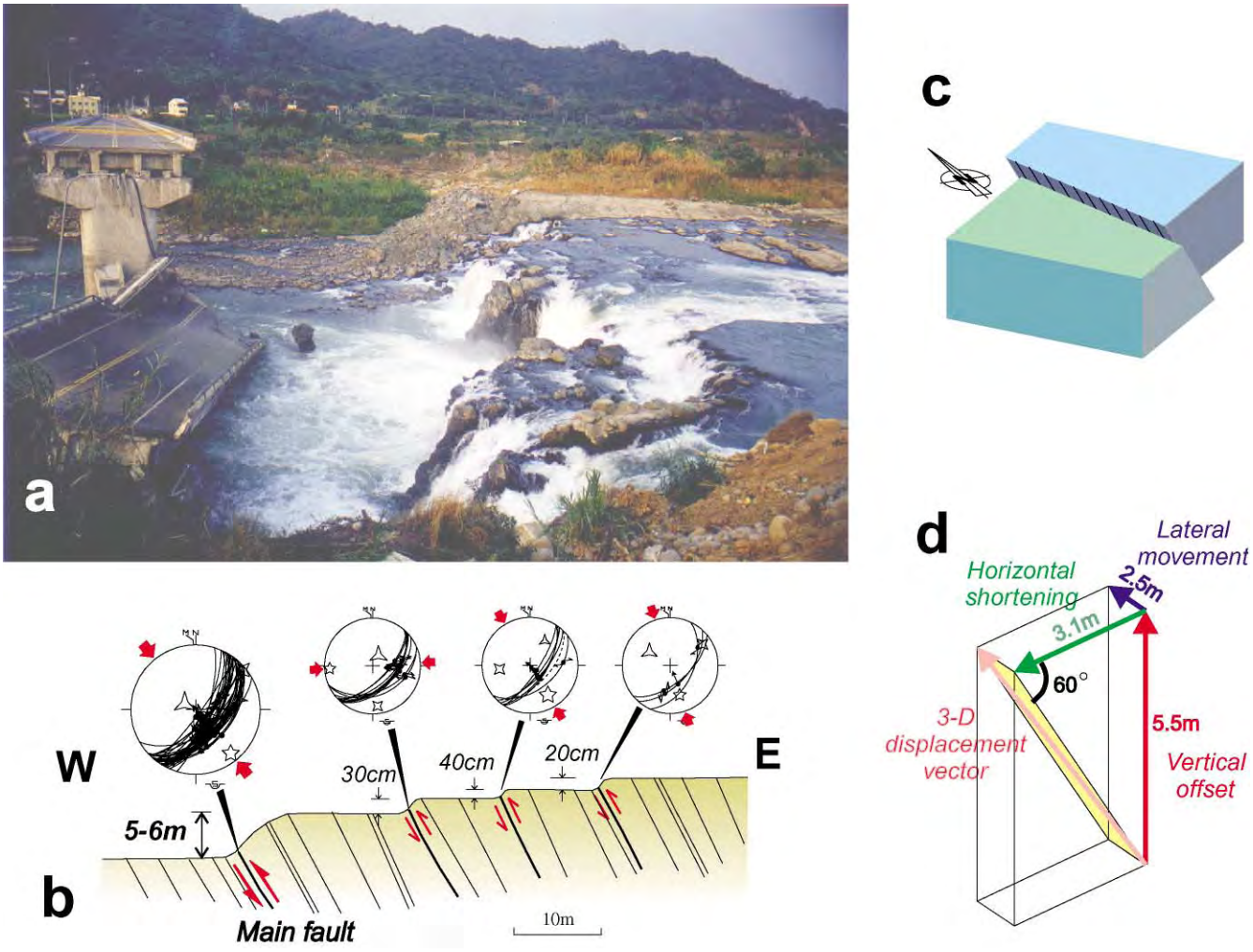

Fig. 8. Kinematics analysis and reconstruction of the movement of the fault in the Pifeng bridge area along the Ta-Chia Chi, near Shihkang. A multi-fault system has been found on the riverbeds and clear striations have been observed on the fault planes and have been measured in order for the kinematics analysis. 3-D reconstruction of the displacement vectors shows that the main fault can be represented by a west-vergent reverse fault (strikes N40°E, dips 60° to SE) with a minor left-lateral strike-slip component.

4. Characteristics of selected sites along the rupture

In this section, we describe structures in selected sites along the rupture. These are used as a basis to support our geometrical reconstruction of the serial cross-sections and the regional kinematic analysis.

4.1. Pifeng Bridge area

On the western side of the northern segment near the Pifeng Bridge (Fig. 6), the surface rupture extended across the active channel of the Ta-Chia Chi ('chi' means river in Chinese) and formed a spectacular waterfall 5–6 m high (Fig. 8a). At least three other 20–40 cm height minor thrusts (Fig. 8b) were also located in the hanging wall of the main surface rupture (i.e. the waterfall). These faults cut 50–60°-dipping strata of the Chinshui Shale parallel to bedding or at a small angle of 10–20°.

Slickenside lineations on the fault planes were observed on the exposed ruptures in the fine-grained sandstone bedrock of the Chinshui Shale. The fault striations revealed dip-slip movements with minor lateral slip for both the main fault and the minor faults. Stress tensor inversions indicate NW–SE directed compression on a NE–SW trending reverse fault dipping to the southeast (Fig. 8b). The stress tensor is generally consistent with the focal mechanism of the main shock of the earthquake (Chung and Shin, 1999; Ma et al., 1999; Kao and Chen, 2000). Note also that it is in a good agreement with the focal solution of the northern sub-event of the main shock (Kao and Chen, 2000). However, a 15–20° clockwise change in the trend of the maximum principal compressive stress direction occurs between the earthquake focus located 50 km to the south and the Pifeng Bridge site. Slip on the main thrust can be illustrated by a 3-D displacement vector (Fig. 8d) with a vertical offset of 5.5 m, a horizontal shortening of 3.1 m, and a small amount of left-lateral strike-slip of 2.5 m. The main fault in the Pifeng area strikes N40°E and dips to the

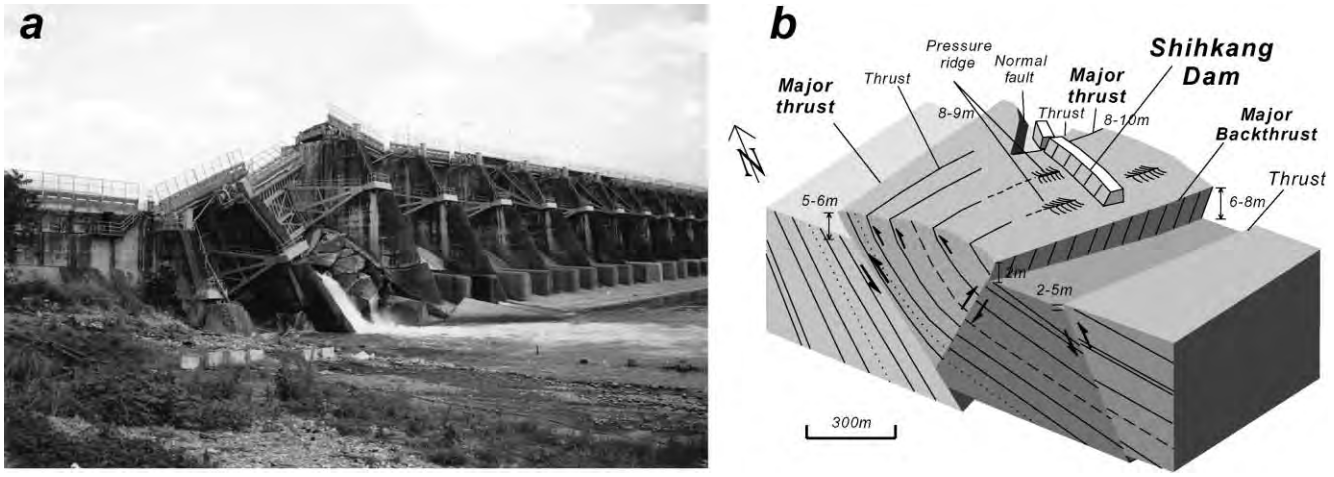

Fig. 9. Complex deformation and fault system in the Shihkang Dam area. (a) Photograph of the Shihkang Dam showing the breaks of the dam body with a vertical offset of 8–10 m. (b) A 3-D block-diagram of the deformation in the Shihkang Dam area. The Shihkang Dam is located on the pop-up fold lifted by thrust and backthrust. At least two thrusts situated on the northern end of the dam have broken the dam. The rest of the dam body has been folded and several different scales of pressure ridges can be observed along the foot of the dam.

east at about 60°; the hanging wall block of the fault moved in the direction of N320°E.

4.2. Shihkang area

4.2.1. Shihkang Dam

Farther east in Shihkang, a system of multiple thrusts and one major backthrust slipped during the earthquake. First, to north of Shihkang in the Ta-Chia Chi, two thrust faults ruptured across through the northern part of Shihkang Dam (Fig. 9). A major thrust, linked to the main thrust analysed at the Pifeng Bridge to the west, exhibited a large vertical displacement of 8–10 m (according to the offset of the dam crest, Fig. 9). The Shihkang Dam is located in the bottom of a triangle zone, whose two edges were formed by a major thrust and a major backthrust. The thrust and the backthrust extend south of the Pifeng Bridge area and gradually increase in displacement on the both sides of the Shihkang Dam (Fig. 9). At least two major thrusts have been found to be closely associated with the destruction of the dam (Chen et al., 2000; Lee et al., 2001). The N–S trending main body of the dam has been folded as a gentle anticline. This N–S to NNW–SSE compression deformation was also reflected by a series of outcrop-scale pressure ridges at the foot of the dam (Fig. 9).

4.2.2. Shihkang

A major backthrust that overlaps the backthrust on the main segment extends in an E–W direction towards the village of Shihkang (Fig. 6). At the western tip of the backthrust, the deformation was accommodated along several ruptures with vertical offsets of 0.5–2 m. At the eastern tip of the backthrust, the surface ruptures formed a single major thrust scarp of 5–6 m high, which closely followed a pre-existing topographic scarp along the southern bank of the Ta-Chia Chi. East of a narrow overlap zone with the major backthrust, another large thrust ruptured the ground surface in an E–W direction for about 3 km in length. The vertical throw of this major thrust varies from 2 to 6 m.

Another kinematic indicator of fault slip was exposed at Shihkang where the hanging wall of the thrust was bisected by a deeply buried support column (Fig. 10). The trace of the tear in the hanging wall block is oriented N5°W on a thrust striking N80°W. For this location, the thrust had a nearly pure dip slip component with only a minor dextral strike slip component.

4.3. Shihcheng area

Three large surface faults can be found in a deformation zone of about 2 km wide east of Shihcheng (Fig. 6). Two west-vergent thrusts are situated on the northwest side of the zone with an east-vergent backthrust on the southeast side. The west-vergent thrusts trend ENE–WSW while the east-vergent thrusts trends NE–SW. The vertical throw of the faults is commonly more than 2 m and as much as 6 m in some places (Fig. 6).

4.4. Cholan-Neiwan area

Farther northeast in the Cholan-Neiwan area, three major surface ruptures were mapped that we interpret as the continuation of the fault segment in the Shihcheng area. Two major NE–SW trending thrusts and one major backthrust, formed in a 2-km-wide fault zone (Fig. 6). The vertical offsets of the individual faults are approximately 1, 1.5, and 5–6 m for the two major thrusts and the major backthrust (respectively, from west to east).

The thrust-and-backthrust surface fault system produced in a distinct pop-up structure in the Neiwan area (Fig. 11),

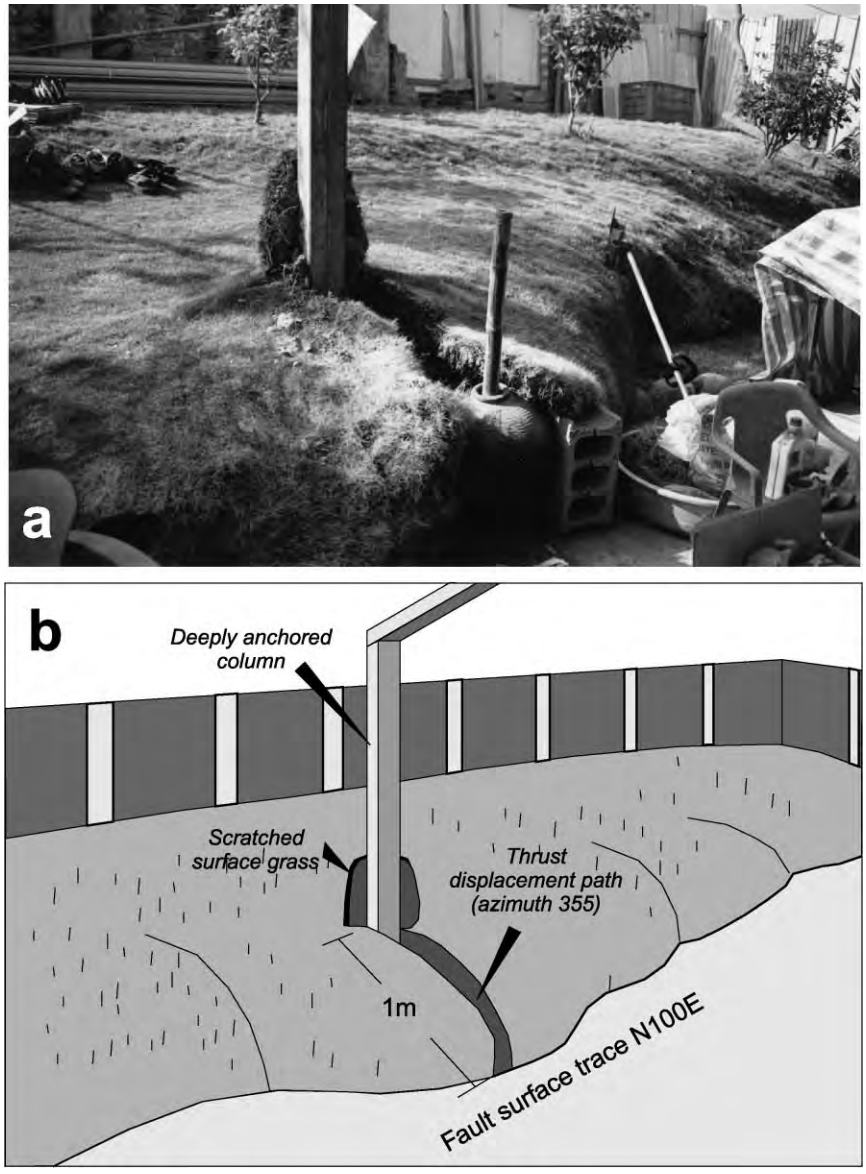

Fig. 10. Photograph (a) and interpretation (b) showing measurement of the fault displacement path on thrust scarp near Shihkang. The earthquake fault went along the backyard and the grass field has been uplifted and moved toward the house during the earthquake. The deeply buried column made a shadow when the soft grass-soil layer went across it. The shadow can be treated as the displacement path of fault in the horizontal plane.

whose margins correspond closely to two limbs of a pre-existing anticlinal fold structure, the Diaoshenshan anticline. The west-vergent surface rupture is situated within the backlimb of the anticline. In some places, the thrust fault did not emerge to the surface level and instead was exposed as fold scarps that formed surface warping, with a height as large as 4 m. The east-vergent backthrust is located on the forelimb of the anticlinal fold. The surface trace of the backthrust followed the topographic expression of a small valley in the Diaoshenshan area. A pre-existing fault zone has been observed on this backthrust zone, which exhibited complicated folded beds and several outcrop-scale minor faults indicating significant shear deformation predating the earthquake.

Several west-vergent minor thrusts parallel to the main faults occurred in the hanging wall adjacent to the major backthrust and are revealed by scarps 15–150 cm high. Tension cracks, oriented sub-parallel to the trend of the surface faults, were common on the hanging wall of the main faults.

Fault striations associated with the surface faulting of the 1999 earthquake were observed in the fault zone of the major backthrust, which produced thrust scarps approximately 5–6 m high. Tensor analysis indicates that the movement of this major backthrust was nearly pure dip-slip. The movement of the major backthrust can be illustrated by a displacement vector with a vertical offset of 5–6 m and a horizontal shortening of 4–5 m. The fault strikes N55°E and dips to the west of about 50°; the hanging wall of the fault moved in the direction of N145°E.

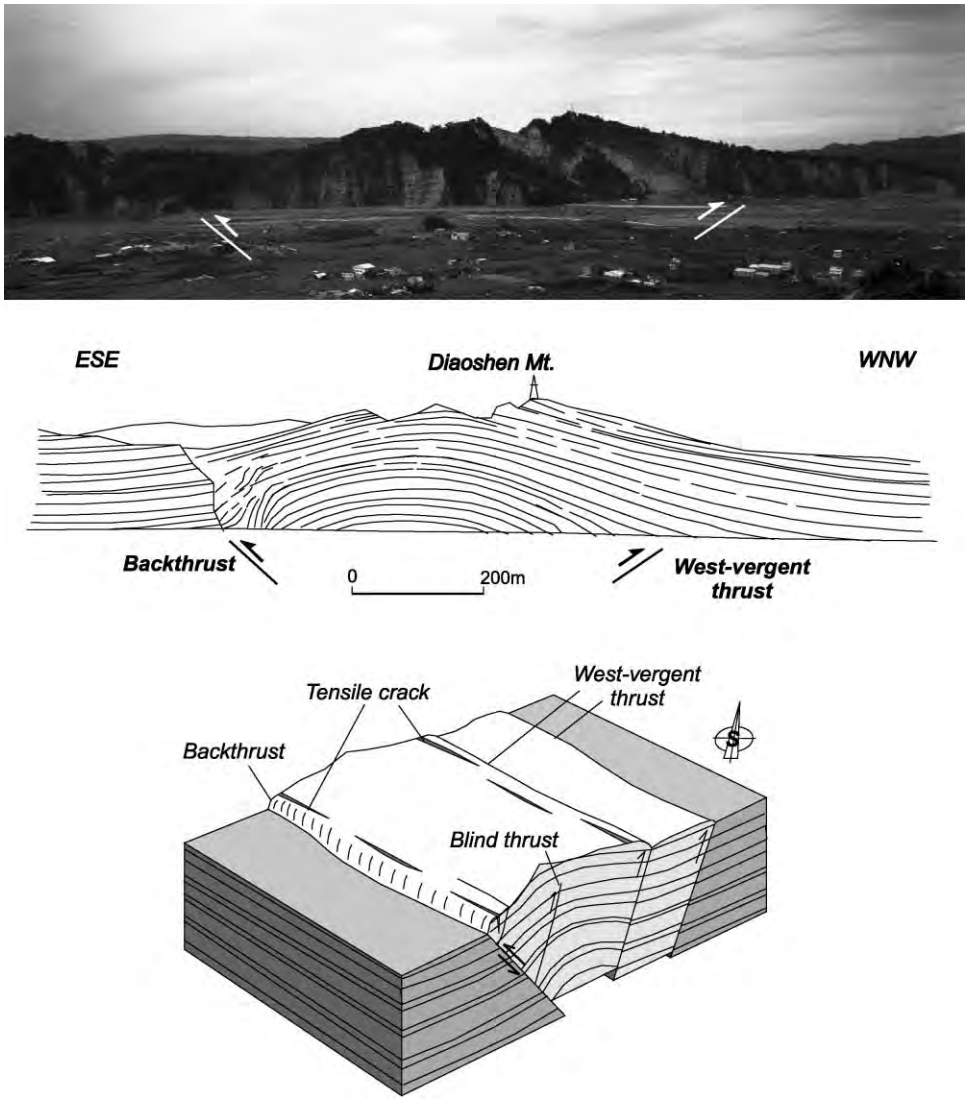

Fig. 11. Pop-up structure with thrust-and-backthrust system situated on a pre-existing anticlinal fold in the Diaoshenshan area near Neiwan. The major thrust of the 1999 earthquake occurred along the backlimb of the Diaoshenshan anticlinal fold and the major backthrust occurred on the forelimb of the anticline. The gentle open fold of the Diaoshenshan implies a young developing anticline, which is probably part of a contribution of several recent earthquakes in a time span of tens of thousand years.

4.5. Shangchi area

To the easternmost part of the northern surface ruptures, the surface faults turned abruptly to a NW–SE strike before they terminated in the Shangchi area (see general geological map in Fig. 4). In this area, the surface ruptures offset west-dipping strata of the Chinshui Shale and were generally parallel or sub-parallel to the bedding plane. Fault striae on the surface ruptures in the northern part of this sub-segment indicate strike-slip component across the fault (Fig. 12a). Shortening was mainly accommodated, however, by dip-slip displacement across surface ruptures that comprise a 300-m-wide zone (Fig. 12b).

Surface ruptures were represented by a major strike-slip fault at the northern end of the Shangchi area. The fault is oriented N–S and dips 70°W and cuts across bedding at a high angle. An offset road indicated about 2 m of dextral slip. Nearly horizontal striae on the fault surface indicate strike-slip displacement (Fig. 12a).

Following the major fault farther southeast near the Ta-An Chi, the trend of surface ruptures turned to NW–SE, parallel to the trend of the bedding planes. The surface faults were characterised by multiple surface ruptures including thrusts and normal faults. On the southern part of this area, a relatively complex pattern of surface faults occurred and followed the NW–SE trending stream of the Kuanyin valley (Fig. 12b). During the earthquake, several pressure ridges and grabens developed along the valley, forming en échelon patterns. Substantial vertical movement (as large as 3 m) occurred along this bedding-parallel structure-controlled valley. Geologically, this area of surface faults is located on the eastern side of the syncline folding

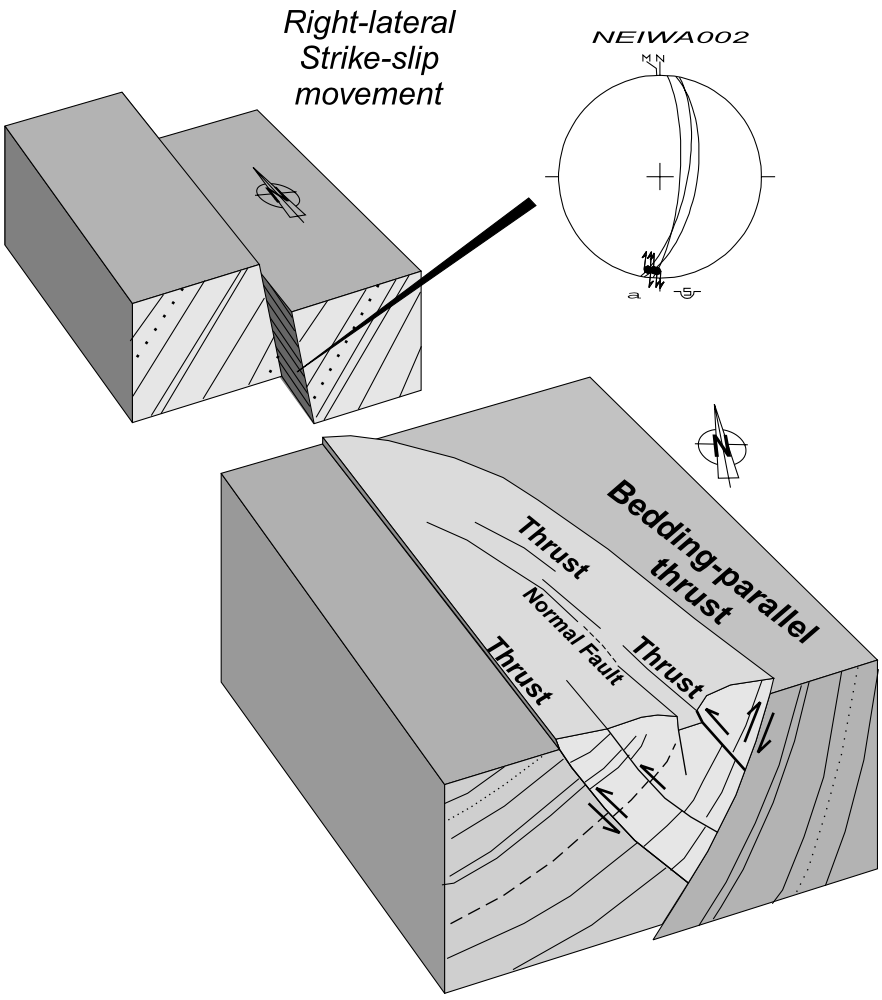

Fig. 12. Simplified block diagrams showing the deformation structure in the eastern part of the Shihkang–Shangchi fault zone. Upper one shows a right-lateral strike-slip movement observed in the outcrop with clear horizontal striations on nearly vertical fault plane. Lower one illustrates a relatively complicated fault system with major bedding-parallel thrust, several antithetic thrusts and normal fault.

Pliocene strata, which has been offset by the Tamaopu Fault (see the geological map in Fig. 4). The Pliocene strata are folded from gentle dips of 10–20° to as much as 70° in a short distance within the 200-m-wide Kuanyin valley. The surface ruptures were discontinuous and showed a complex pattern that we interpret as related to the nature of loosely consolidated conglomerate in the bed of the river. In general, two arch-like structures showed both compressive and extensional folding and faulting. This led to different interpretations of the surface ruptures in the Kuanyin valley (e.g. normal faulting for Lin et al. (1999)). The vertical offset of the faults varies from 1 to 3 m.

5. Serial cross-section

Serial cross-sections have been constructed (Fig. 13) in order to illustrate the along-strike evolution of the major structures and the change in fault geometry along the surface rupture in the northern segment of the Shihkang–Shangchi area. Our reconstruction of cross-sections is based mainly on both the detailed outcrop investigations along the rupture zone presented above and subsurface data such as oil wells and seismic reflection profiles that define the underlying geological structure. Again we note that the northern surface ruptures developed in a large syncline on both limbs within the Chinshui shale. Within the syncline, the surface ruptures developed along small anticlinal folds, which sometimes post-dated and overprinted the regional large synclinal structure. For instance, surface pop-up ruptures following the Diaoshenshan anticline, which trends NE–SW, cut obliquely through the N–S trending regional syncline axis (Fig. 13).

The western end (section AA′, Fig. 13) illustrates the typical structure of the main segment of the surface ruptures. The earthquake slip runs along the range-front and results from reactivation of the boundary fault, along which Pliocene marine sediments of shale or fine-grained sandstone (generally Chinshui Shale) were thrusted over Quaternary deposits. In cross-section, the earthquake fault

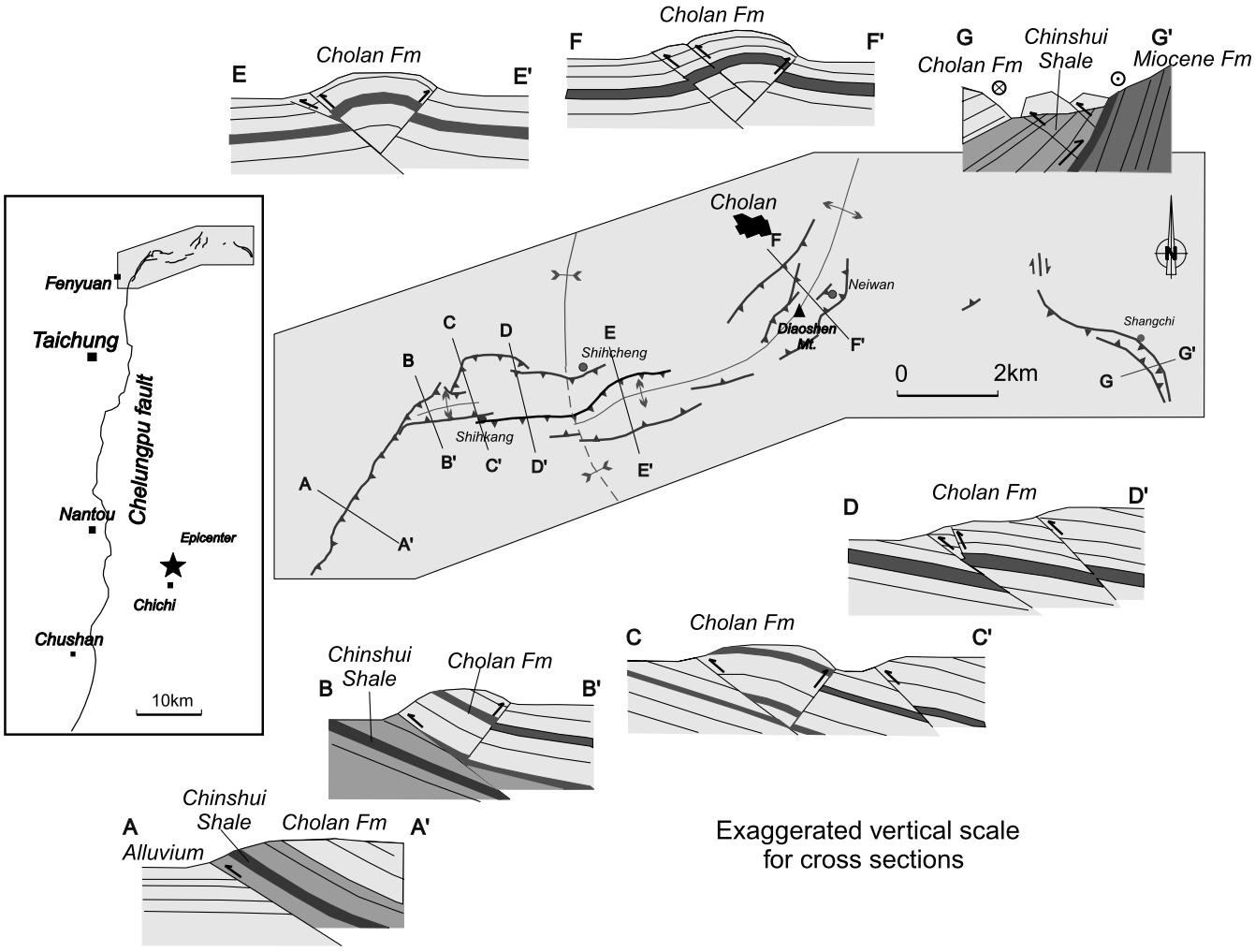

Fig. 13. Serial cross-section along the Shihkang–Shangchi fault zone. Seven representative cross-sections from west to east have been shown in order to illustrate the characteristics and change of structural feature along the fault zone. AA′ represents the general feature in the main segment of the Chelungpu fault. BB′, CC′, and DD′ represent the feature on the western side of the fold axis of the regional Cholan syncline. EE′ and FF′ represent the structure on the central-eastern side of the Cholan syncline. GG′ represents the structure in the easternmost part. Detailed structural characteristics for each cross-section seen in the text.

extends parallel or slightly oblique to bedding in Pliocene strata, which dip 30° east in an elongate monocline interpreted as the backlimb of a fault-bend fold formed previously above the ancestral Chelungpu thrust. Farther to the northeast, in the Pifeng Bridge area, the section BB′ illustrates a characteristic pop-up structure, with a NW-verging thrust and a backthrust. To the east, the surface traces rotated clockwise into foothills and did not follow the topographic boundary of the foothills and the coastal plain. Instead, they cut across the Pilocene Cholan Formation. Note that the NW-vergent thrust acted as a bedding-parallel thrust, whereas the backthrust cut across bedding at a high angle. To the east, in the Shihkang area, the section CC′ shows another NW-vergent major thrust that developed behind the pop-up structure mentioned above. This west-vergent thrust cut across bedding in Cholan Formation (above the Chinshui Shale). Farther east, the section DD′ is located in a transition zone between two pop-up structures. In this cross-section, two major NW-vergent thrusts developed, neither of which was bedding-parallel. The EE′ and FF′ sections show an earthquake-related pop-up structure developing in the pre-existing Diaoshenshan anticline. Two major west-vergent thrusts appeared on the northwest limb of the fold, and a backthrust developed on the other side of the fold. It is worth noting that folds with gently dipping strata on the limbs indicate that the folds are geologically young and thus active structures. As noted before, the clear topographic expression of the Diaoshenshan anticline axis above the average surface of the rapidly eroded Pliocene syncline (see DEM image in Fig. 5) indicates that this gentle anticline probably grew during the recent times. The last cross-section GG′ shows that the earthquake fault spin in a complex rupture pattern to the northeast. The surface ruptures turned clockwise to follow the regional trend of strata. Near the eastern tip of the fault zone, the surface ruptures extended into the

Chinshui Shale and became a bedding-parallel thrust. This situation is quite similar to that already described on the western side of the syncline (e.g. AA′ and BB′). In the GG′ area, the northern sub-segment showed a right-lateral strike-slip fault, whereas the southern sub-segment revealed a major bedding-parallel backthrust and several secondary west-vergent thrusts, as well as a few normal faults.

In summary, thrust scarps with pop-up uplift folds prevailed along the surface ruptures in the SSFZ. Despite a large variety of situations and offsets along the fault zone from west to east, two opposing factors played a major role at the hectometric-kilometric scale. The presence of mechanical anisotropy related to stratigraphy resulted in bedding-parallel faulting, whereas the basement-controlled fault obliquity (relative to pre-existing structures) resulted in complicated patterns of across-bedding faults, fractures and folds in the upper sedimentary layers. Bedding-parallel thrusts ruptured both sides of the SSFZ (NW-vergent thrust on the west and E-vergent thrust on the east), whereas thrusts and backthrusts that cross cut bedding are located in the middle part of the fault zone. The displacements of the west-vergent thrusts are larger than the east-vergent backthrusts on the western side of the northern segment. This difference in the amounts of displacement for thrusts and backthrusts decreases toward the east along the zone of surface ruptures. In the middle and eastern parts of the northern segment, the backthrusts exhibited displacements equal to, or even larger than, those of the west-verging thrusts. To the east, the complexity increases because of right-lateral slip on N–S oriented strike-slip faults. As a result, the relative horizontal displacement across the earthquake fault zone is accommodated in different ways and gradually from west to east. The total vertical displacement, however, did not change significantly from west to east and remained high (4–6 m on average) all along the northern surface ruptures.

6. Kinematic model

The surface ruptures of the 1999 Chi-Chi earthquake reached their largest displacement near the junction between the main N–S trending segment of the Chelungpu fault and the NE–SW/ENE–WSW trending northern segment (the SSFZ), and terminated farther to the northeast (see GPS data in Fig. 3). In order to illustrate the structural characteristics of the SSFZ, we developed a kinematic model with 3-D earthquake fault configuration. We first compile kinematic data including seismological analysis of earthquake rupturing, coseismic GPS measurements, and our field investigation and kinematic analysis. We then propose a 3-D fault framework and illustrate its relationship with the regional structural and geological inheritance.

6.1. General kinematics features

Seismic inversion studies of the rupturing process of the Chi-Chi earthquake (Kikuchi et al., 2000; Lee and Ma, 2000; Ma et al., 2000) indicate that the earthquake initiated in the south and that the surface rupture propagated toward the north along the Chelungpu fault. The distribution of the displacement of the major fault plane of the Chi-Chi earthquake has been modelled based on seismological analysis (Kikuchi et al., 2000; Ma et al., 2000). It revealed that the

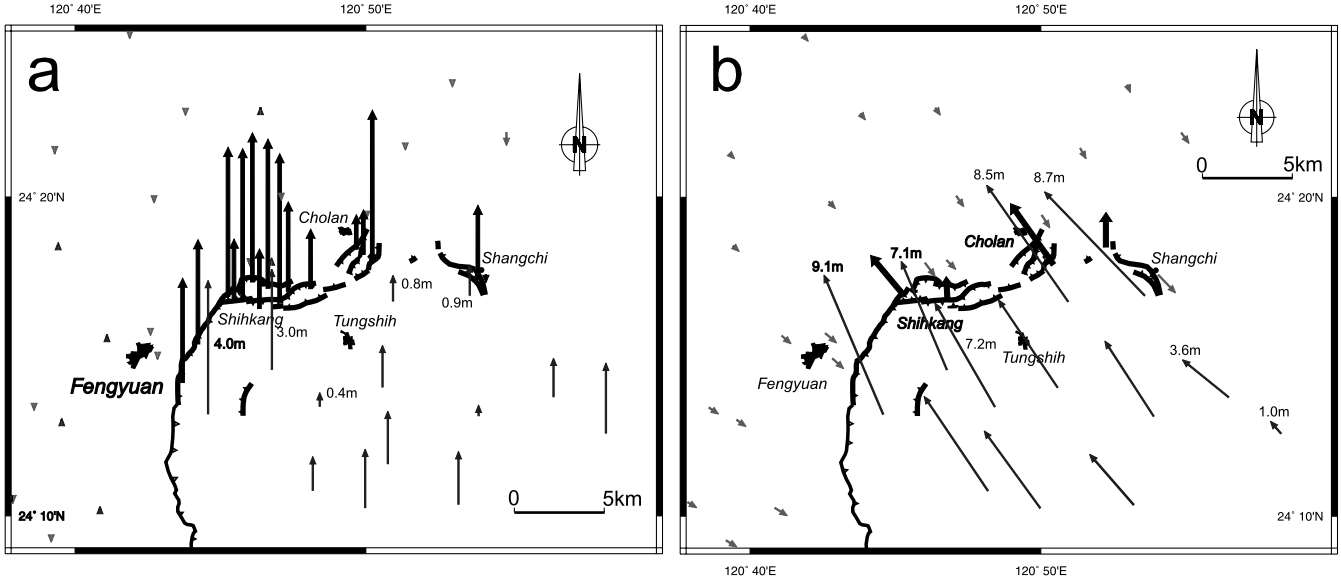

Fig. 14. Co-seismic movement of the 1999 Chi-Chi earthquake from GPS (thin arrows) and field outcrop (heavy arrows) measurements in vertical (a) and horizontal (b) components. Substantial vertical displacement is focused on the narrow zone along the pop-ups in the Shihkang–Shangchi fault zone. The vertical and horizontal co-seismic displacement data indicate that the surface fault of the northern termination reveals a thrust behaviour in terms of fault motion. GPS data sources come from Central Geological Survey (1999b) and Yu et al. (2001).

displacement of the earthquake fault increased from the hypocentre northward and reached a maximum value of at least 7 m about 40–50 km north of the hypocentre. GPS measurements also show that the near-surface co-seismic displacement increased gradually along the Chelungpu fault zone, from 2–3 m near the epicentre area to approximately 7–9 m in the north (Central Geological Survey, 1999a; IES, 1999; Yang et al., 2000; Yu et al., 2001). The surface fault displacement of the earthquake changed and diminished dramatically within a relatively short distance along the northern surface ruptures of the SSFZ.

Co-seismic GPS measurements in the SSFZ (Fig. 14) indicate that displacements across the surface fault remained generally large all along the rupture zone until the easternmost portion where the displacement diminished dramatically. The distribution of the vertical displacement revealed by the GPS analysis (Fig. 14a) indicates that vertical separation across the hanging wall block decreased from west (3–4 m) to east (<1 m) and died out around Shangchi. Minor subsidence (<0.1 m) occurred on the footwall block. The horizontal component of GPS co-seismic displacement remains large (7–9 m) for the hanging wall block relative to the footwall block (Fig. 14b). The horizontal component of displacement of the hanging wall block varies from a vector of N23°W to the west, to N45°W to the east (Fig. 14b). The horizontal displacements diminished dramatically in a short distance around Shangchi.

Field outcrop measurement of fault movement (Table 1 and Fig. 14) reveals that the earthquake fault displacement remained large along the northern surface ruptures, from west to east (Pifeng Bridge to Shangchi). Surface displacement was largely accommodated by conjugate reverse faulting on NE-verging thrusts and SW-verging backthrusts. Field observation shows that the vertical uplift was generally higher than the horizontal shortening component on the reverse faults. Vertical uplift in the SSFZ was not only accommodated by reverse faulting, but also by co-seismic uplift of fault-related folds. Furthermore, comparing the GPS data, we note that the vertical movement associated with the 1999 earthquake is confined to a 1–2-km-wide rupture zone for the northern segment, whereas it is distributed across a relatively wider zone for the main segment.

Combining field and GPS displacement data (Fig. 14), we note that displacement is mostly concentrated on a narrow zone along the surface uplift pop-ups bounded by thrust and backthrust scarps. In addition, horizontal displacement from both the GPS data and the outcrop measurements indicate that the northernmost segment behaves dominantly as a thrust fault.

6.2. Three-dimensional kinematics

We propose a kinematic model to illustrate the regional structure of the northern surface ruptures (Fig. 15). Fig. 15 shows a 3-D block diagram of major structures in the area of northern termination of the 1999 Chi-Chi earthquake ruptures. The major structures include the Chelungpu fault, the south-plunging regional syncline, the SSFZ, the Sanyi fault, and the Tamaopu fault. The faults are shown on the diagram to illustrate their geometric relationship during the earthquake. For instance, the Sanyi fault merges into the northern Chelungpu fault and the SSFZ, while the Tamaopu fault cuts through the SSFZ.

Based on the above geological analysis and available geophysical information, we propose that the fault plane developed principally within the Chinshui Shale and parallel to bedding of the hanging wall strata for the uppermost 2–3 km. A close geometric correlation exists between

Table 1
Results of kinematics analysis from the outcrop in-site measurements on the fault scarps of the northern termination of the 1999 Chi-Chi earthquake. Two kinds of analysis have been adopted for this study, including the fault-slip data analysis (Type I) and the restoration of the markers across the thrust scarps (Type II)

No.	Area	Latitude/longitude	Vertical offset (m)	Horizontal shortening (m)	Lateral slip (m)	Fault strike (azimuth)	Fault dip (degree)	Slip direction (azimuth)	Type of measurement
1a	Pifeng Bridge	N24°16.905′ E120°45.123′	5.5	3.1	2.5	040	55–75	320	I
1b	Pifeng Bridge	N24°16.905′ E120°45.123′	0.3	~0.2	–	050	50–65	280	I
1c	Pifeng Bridge	N24°16.905′ E120°45.123′	0.4	~0.25	–	045	50–70	325	I
1d	Pifeng Bridge	N24°16.905′ E120°45.123′	0.2	~0.15	–	045	50–60	350	I
2	Shihkang	N24°16.752′ E120°46.343′	1.5–2	1–2	<0.5	100	–	355	II
3	Shihkang Dam	N24°17.1′ E120°45.67′	1.5	1.2	–	024	50	290–300	II
4	Neiwan	N24°17.384′ E120°48.910′	5–6	4.2–5.0	–	55	50	145	I
5	Shangchi	N24°18.134′ E120°52.54′	<0.5	<0.5	~2	010	60–70	~000	I

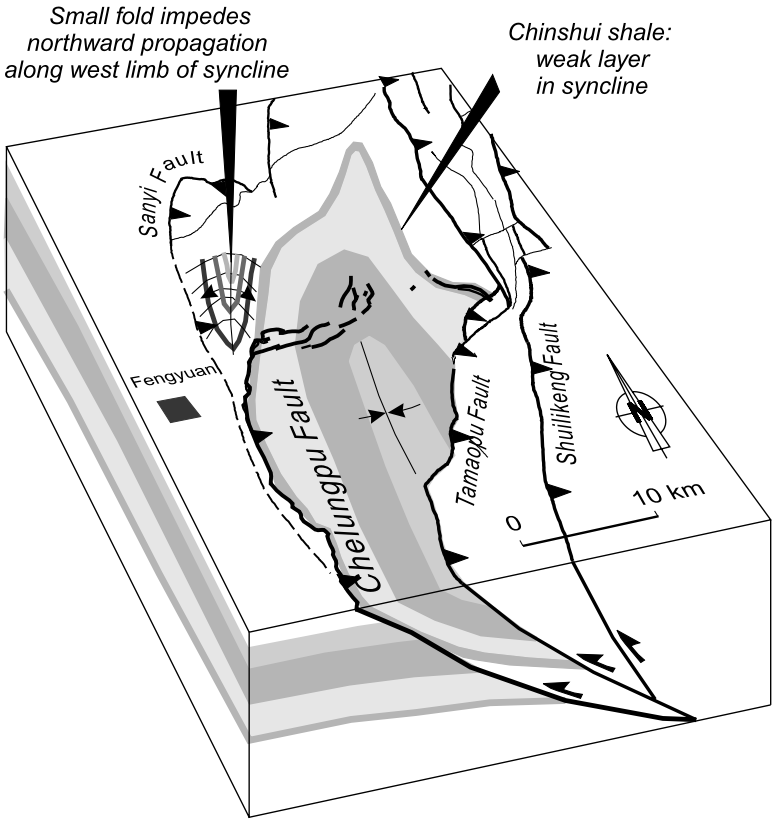

Fig. 15. Geometric configuration of the northern termination of the 1999 earthquake illustrated in a 3-D block diagram. The 1999 Chi-Chi earthquake generally ruptured along the Chelungpu fault and developed parallel to bedding of the weak zone of the Chinshui Shale at the upper 2–3 km. Geological and lithological 3-D geometry show the Chinshui Shale became shallower toward the north. The rupture surface finally emerged to the surface in the Shihkang–Shangchi fault zone and formed a spoon-like shape towards the core of the regional Pliocene syncline. This south-plunging Pliocene syncline acts as a slip guide for the new ongoing Chelungpu thrust (see text for details).

the regional fold structure and the 1999 earthquake fault rupture surface. An east-dipping monocline on the hanging wall of the Chelungpu fault is transformed gradually into a synclinal fold to the northern. As a result, the geometry of the fault plane would be dipping not only to the east, but also gently to the south at the regional scale because of the south-plunging syncline structure (Fig. 15). As the earthquake propagated to the north, the fault plane became shallower near the SSFZ. This model implies that the shape or geometry of the lithological layers controls the northern surface ruptures. In fact, the trend of the northern surface ruptures (spoon-like shape) is generally consistent with the regional trends of bedding. This 3-D model of the fault surface geometry indicates a strong influence of the regional structural inheritance on the earthquake fault development, i.e. the south-plunging syncline acts as a strain guide for the 'new' Chelungpu thrust.

In summary, within the area of the northern surface ruptures, the SSFZ, the surface faults developed within the large south-plunging Pliocene syncline and extended into the Chinshui Shale on both sides of this syncline (Fig. 15). Thus, the 3-D geometry of the earthquake fault surface resembles a half spoon: the left side of the spoon represents the straight N–S trace of the main segment of the Chelungpu fault, while the curved tip of the spoon corresponds to the complex E–W trace to the north. The large Pliocene syncline with a southward-plunging axis acted as a slip/strain guide for the last event of thrusting along the Chelungpu fault. Propagating from the south, the 1999 rupture followed the weakest stratigraphic zone, the Pliocene Chinshui Shale, as an easy-shear channel, so that the trace generally follows the synclinal structure at the near-surface level. Then it broke through the syncline, as the SSFZ. The reason why there is so much vertical displacement on several small discontinuous thrust-backthrust features probably lies in the geometrical requirement for the fault rupture to occur over a surface whose radius of curvature rapidly decreases to the north when approaching the core of the syncline.

7. Conclusions

1. The surface ruptures associated with the 1999 Chi-Chi earthquake display a complex shape as they abruptly turn clockwise in the northern area and enter a broad Pliocene syncline in the foothills. In this region (the Shihkang–Shangchi Fault Zone, SSFZ) the surface ruptures extend

over a length of about 15 km, and they are characterised by a complex structural pattern involving pop-ups bounded by thrust and backthrust and other brittle features forming several en échelon distributed sub-segments.

2. Field investigation and kinematic analysis show that most of the surface ruptures in the SSFZ are dip-slip thrusts with minor strike-slip. This displacement pattern is consistent with the larger-scale GPS co-seismic displacement independently reconstructed. Substantial vertical movements prevailed on thrust scarps and fold scarps, which had a height as much as 8–10 m and left numerous surface damages.
3. On the two extremities of the SSFZ, the surface ruptures slip principally parallel to bedding of the Pliocene Chinshui shale: west-vergent thrusting on the west limb of the regional broad syncline and east-vergent thrusting on the east limb of the syncline. In the middle part of the SSFZ, the pop-ups reactivated the pre-existing Diaoshenshan anticline. As a result, west-vergent thrusts occurred on the backlimb and east-vergent backthrusts occurred within a pre-existing fault zone on the forelimb of the anticline. This NE–SW trending anticline is undergoing an uplift process and it cuts and breaks through the regional N–S trending south-plunging syncline.
4. The distribution and geometry of the northern surface ruptures are closely related to the regional geological and structural inheritance, i.e. the stratigraphy and the regional fold structure. Surface geological information, GPS measurement of co-seismic movement, and subsurface geological/geophysical data indicated that the northern surface rupture developed within the large south-plunging Pliocene syncline and extended down to the weak zone of the Chinshui Shale on both sides of this syncline. We conclude that the weakest layers of the southward-plunging regional Pliocene syncline acted as a slip/strain guide for the new ongoing Chelungpu thrust. Both the larger vertical displacement along the SSFZ and the splitting of the earthquake fault into relatively short segments can be explained by two main structural requirements. One is the decreasing radius of curvature of the weak layer along which the earthquake fault propagated towards the north and northeast. The second requirement deals with the obliquity of the major fold structure in the sedimentary pile, relative to the basement-controlled average displacement vector.

Acknowledgements

Field work was funded by Institute of Earth Sciences, Academia Sinica, National Taiwan University, Central Geological Survey, and National Science Council grants NSC88-2116-M001-037 and NSC89-2116-M001-037. It also benefited from support by the Taiwan–France co-operation frame in Earth Sciences (National Science Council and Institut Français à Taipei). Helpful reviews and suggestions by K. Mueller and J. Spotila greatly improved the manuscript. We wish to thank Z. Shipton for editing this paper in the final stage. This is a contribution of the Institute of Earth Sciences, Academia Sinica, IESEP2001-008.

References

Angelier, J., 1984. Tectonic analysis of fault-slip data sets. Journal of Geophysical Research 89, 5835–5848.

Angelier, J., 1989. From orientation to magnitudes in paleostress determinations using fault slip data. Journal of Structural Geology 11, 37–45.

Angelier, J., 1994. Fault slip analysis and paleostress reconstruction. In: Hancock, P.L. (Ed.), Continental Deformation. Pergamon Press, Oxford, Chap. 4, pp. 53–100.

Angelier, J., Chu, H.T., Lee, J.C., Hu, J.C., Mouthereau, F., Lu, C.Y., Deffontaines, B., Lallemand, S., Tsai, Y.B., Chow, J.D., Bureau, D., 2000. Geological knowledge and seismic risk mitigation: insights from the Chi-Chi earthquake, Taiwan. In: Loh, C.H., Liao, W.I. (Eds.), International Workshop on Annual Commemoration of Chi-Chi Earthquake, vol. I. National Center for Research on Earthquake Engineering, Taipei, pp. 13–24.

Berberian, M., 1979. Earthquake faulting and bedding thrust associated with the Tabas-e-Golshan (IRAN) earthquake of September 16, 1978. Bulletin of Seismological Society of America 69 (6), 1861–1887.

Bilham, R., Yu, T.T., 1999. The morphology of thrust faulting in the 21 September 1999, Chichi, Taiwan earthquake. Journal of Asian Earth Sciences 18, 351–367.

Biq, C., 1972. Western Taiwan thrusts, active? or inactive? Acta Geologica Taiwanica 15, 63–76.

Central Geological Survey, 1999. Map of surface ruptures along the Chelungpu fault during the Chi-Chi earthquake, Taiwan scale 1:25,000, Central Geological Survey, MOEA, Taipei.

Central Geological Survey, 1999. Report of the geological survey of the 1999 Chi-Chi earthquake (in Chinese). Central Geological Survey, Taipei.

Chang, S.S.L., 1971. Subsurface geologic study of the area from the Taipei basin to the Kuanyin shelf, Taoyuan, Taiwan. Petroleum Geology of Taiwan 9, 123–144.

Chang, C.H., Wu, Y.M., Shin, T.C., Wang, C.Y., 2000. Relocation of the 1999 Chi-Chi Earthquake in Taiwan. Terrestrial, Atmospheric and Oceanic Sciences 11 (3), 581–590.

Chen, W.C., Chu, H.T., Lai, T.C., 2000. Surface ruptures of the Chi-Chi Earthquake in the Shihgang Dam area. Special Issue on the Chi-Chi Earthquake, 1999. Central Geological Survey Spec. Publ. 12, 41–62.

Chou, J.T., 1971. A sedimentologic and paleogeographic study of the Neogene formations in the Taichung region, Western Taiwan. Petroleum Geology of Taiwan 9, 43–66.

Chung, J.K., Shin, T.C., 1999. Implication of the rupture process from the displacement distribution of strong ground motions recorded during the 21 September 1999 Chi-Chi, Taiwan earthquake. Terrestrial, Atmospheric and Oceanic Sciences 10 (4), 777–786.

Chinese Petroleum Corporation, 1974. Geological map of Miaoli, Chinese Petroleum Corporation, scale 1:100,000. Chinese Petroleum Corporation.

Chinese Petroleum Corporation, 1982. Geological map of Taichung, Chinese Petroleum Corporation, scale 1:100,000. Chinese Petroleum Corporation.

Elishewitz, B., 1963. A new interpretation of the structure of the Miaoli area in the light of the decollement tectonics of northwest Taiwan. Petroleum Geology of Taiwan 2, 21–45.

Ho, C.S., 1967. Structural evolution of Taiwan. Tectonophysics 4, 367–378.

Ho, C.S., 1975. An introduction to the geology of Taiwan: explanatory text of the geologic map of Taiwan. Ministry of Economic Affairs, ROC.

Ho, C.S., 1976. Foothill tectonics of Taiwan. Bulletin of Geological Survey of Taiwan 25, 9–28.

Ho, C.S., 1986. A synthesis of the geologic evolution of Taiwan. Tectonophysics 125, 1–16.

IES, 1999. Institute of Earth Sciences The Chi-Chi Earthquake in Taiwan. http://www.earth.sinica. edu.tw/921/921chichi_main_eng.htm.

Kao, H., Chen, W.P., 2000. The Chi-Chi earthquake sequence: active out-of-sequence thrust faulting in Taiwan. Science 288, 2346–2349.

Kikuchi, M., Yagi, Y., Yamanaka, Y., 2000. Source process of the Chi-Chi, Taiwan, earthquake of September 21, 1999 inferred from teleseismic body waves. Bulletin of Earthquake Research Institute of University Tokyo 75 (1), 1–14.

Lee, S.J., Ma, K.F., 2000. Rupture process of the 1999 Chi-Chi, Taiwan, earthquake from the inversion of teleseismic data. Terrestrial, Atmospheric and Oceanic Sciences 11 (3), 591–608.

Lee, J.C., Lu, C.Y., Chu, H.T., Delcaillau, B., Angelier, J., Deffontaines, B., 1996. Active deformation and paleostress analysis in the Pakua anticline area, western Taiwan. Terrestrial, Atmospheric and Oceanic Sciences 7 (4), 431–446.

Lee, J.C., Angelier, J., Chu, H.T., Hu, J.C., Chan, Y.C., Lu, C.Y., 2001. Characteristics of the surface and kinematic analysis of the Chi-Chi earthquake, September 21 1999, Taiwan. Tectonics, submitted.

Lin, C.-W., Lai, W.-C., Huang, M.-L., Liou, Y.-C., Wu. M.-C., Hsieh, C.-L., 1999. Earthquake cause and faulting mechanism of the 921 Earthquake (in Chinese). In: Report of the 921 Chi-Chi Earthquake Investigation. National Center for Research on Earthquake Engineering, Taipei.

Ma, K.-F., Lee, C.T., Tsai, Y.B., Shin, T.C., Mori, J., 1999. The Chi-Chi, Taiwan earthquake: large surface displacements on an inland thrust fault. EOS, Transactions 80 (50), 605–611.

Ma, K.-F., Song, T.-R.A., Lee, S.-J., Wu, H.-I., 2000. Spatial slip distribution of the September 20, 1999, Chi-Chi, Taiwan, earthquake (Mw7.6) — inverted from teleseismic data. Geophysical Research Letter 27 (20), 3417.

Mouthereau, F., 2000. Evolution structurale et Cinematique recente a actuelle de l'avant-pays plisse d'une chaine de collision oblique: Taiwan. Unpublished Mem. Sc. Terre thesis, Univ. P.-et-M. Curie.

Mouthereau, F., Deffontaines, B., Lacombe, O., Angelier, J., 2001. Along-strike variations of the Taiwan belt front: basement control on structural style, wedge geometry and kinematics. Geological Society of America Special Paper, in press.

Mueller, K., Suppe, J., 1997. Growth of Wheeler Ridge anticline, California: geomorphic evidence for fault-bend folding behaviour during earthquakes. Journal of Structural Geology 19 (3–4), 383–396.

Namson, J., 1981. Structure of the western foothills belt, Miaoli–Hsinchu area, Taiwan. Petroleum Geology of Taiwan 18, 31–51.

Philip, H., Meghraoui, M., 1983. Structural analysis and interpretation of the surface deformations of the El Asnam earthquake of October 10, 1980. Tectonics 2 (1), 17–49.

Philip, H., Rogozhin, E., Cisternas, A., Bousquet, J.C., Borisov, B., Karakhanian, A., 1992. The Armenian earthquake of 1988 December 7: faulting and folding, neotectonics and palaeoseismicity. Geophysical Journal Interior 110, 141–158.

Shaw, J., Shearer, P., 1999. An elusive blind-thrust fault beneath Metropolitan Los Angeles. Science 283, 1516–1518.

Sieh, K.E., Jahns, R.H., 1984. Holocene activity of the San Andreas fault at Wallace Creek, California. Bulletin of Seismological Society of America 95, 883–896.

Stein, R., King, G., 1984. Seismic potential revealed by surface folding: 1983 Coalinga, California Earthquake. Science 224, 869–872.

Suppe, J., 1980. Imbricated structure of western foothills belt, south-central Taiwan. Petroleum Geology of Taiwan 17, 1–16.

Suppe, J., 1981. Mechanics of mountain building in Taiwan. Memoir Geological Society of China 4, 67–89.

Tsutsumi, Y., Yeats, R., 1999. Tectonic setting of the 1971 Sylmar and 1994 Northridge earthquakes in the San Fernando Valley, California. Bulletin of Seismological Society of America 89 (5), 1232–1249.

Yang, M., Rau, R.-J., Yu, J.-Y., Yu, T.-T., 2000. Geodetically observed surface displacements of the 1999 Chi-Chi, Taiwan, earthquake. Earth Planets Space 52, 403–413.

Yeats, R.S., Sieh, K.E., Allen, C.R., 1997. The Geology of Earthquakes. Oxford University Press, New York.

Yu, S.B., Kuo, L.C., Su, H.H., Liu, C.C., Hou, C.S., Lee, J.F., Lai, T.C., Liu, C.C., Liu, C.L., Tseng, T.F., Tsai, C.S., Shin, T.C., 2001. Preseismic deformation and coseismic displacements associated with the 1999 Chi-Chi, Taiwan earthquake. Bulletin of Seismological Society of America, in press.